PHILOSOPHICAL TRANSACTIONS OF THE ROYAL SOCIETY B

rstb.royalsocietypublishing.org

Research

Cite this article: Dandekar SN, Park JS, Peng GE, Onuffer JJ, Lim WA, Weiner OD. 2013 Actin dynamics rapidly reset chemoattractant receptor sensitivity following adaptation in neutrophils. Phil Trans R Soc B 368: 20130008. http://dx.doi.org/10.1098/rstb.2013.0008

One contribution of 17 to a Discussion Meeting Issue 'Cellular polarity: from mechanisms to disease'.

Subject Areas:
cellular biology

Keywords:
actin, receptor, neutrophil, adaptation, cell polarity, chemotaxis

Author for correspondence:
Orion D. Weiner
e-mail: orion.weiner@ucsf.edu

Electronic supplementary material is available at http://dx.doi.org/10.1098/rstb.2013.0008 or via http://rstb.royalsocietypublishing.org.

Royal Society Publishing
Informing the science of the future

Actin dynamics rapidly reset chemoattractant receptor sensitivity following adaptation in neutrophils

Sheel N. Dandekar[1,6], Jason S. Park[2,3,4], Grace E. Peng[5], James J. Onuffer[2,4], Wendell A. Lim[2,3,4] and Orion D. Weiner[5,6]

[1]Department of Biophysics, [2]Cellular and Molecular Pharmacology, [3]Howard Hughes Medical Institute, [4]The Cell Propulsion Lab, and [5]Department of Biochemistry, Genentech Hall, University of California, 600 16th Street, San Francisco, CA 94158, USA
[6]Cardiovascular Research Institute, SCVRB Room 384, University of California, 555 Mission Bay Boulevard South, San Francisco, CA 94158, USA

Neutrophils are cells of the innate immune system that hunt and kill pathogens using directed migration. This process, known as chemotaxis, requires the regulation of actin polymerization downstream of chemoattractant receptors. Reciprocal interactions between actin and intracellular signals are thought to underlie many of the sophisticated signal processing capabilities of the chemotactic cascade including adaptation, amplification and long-range inhibition. However, with existing tools, it has been difficult to discern actin's role in these processes. Most studies investigating the role of the actin cytoskeleton have primarily relied on actin-depolymerizing agents, which not only block new actin polymerization but also destroy the existing cytoskeleton. We recently developed a combination of pharmacological inhibitors that stabilizes the existing actin cytoskeleton by inhibiting actin polymerization, depolymerization and myosin-based rearrangements; we refer to these processes collectively as actin dynamics. Here, we investigated how actin dynamics influence multiple signalling responses (PI3K lipid products, calcium and Pak phosphorylation) following acute agonist addition or during desensitization. We find that stabilized actin polymer extends the period of receptor desensitization following agonist binding and that actin dynamics rapidly reset receptors from this desensitized state. Spatial differences in actin dynamics may underlie front/back differences in agonist sensitivity in neutrophils.

1. Introduction

Chemotaxis is the process by which cells direct their movements along an extracellular chemical gradient of an agonist. Many vital processes require chemotaxis, such as axonal guidance, patterning of developing embryos and pathogen detection by the innate immune system, including human neutrophils. In neutrophils, agonist binding to chemotactic receptors triggers a set of signalling pathways to generate polarized actin polymerization that drives chemotaxis. Several signal processing capabilities are required for chemotaxis. Adaptation allows neutrophils to respond to relative changes rather than steady-state concentrations of ligand, enabling them to migrate up chemotactic gradients spanning several orders of magnitude [1,2]. Neutrophils also generate a consistent internal polarity that does not depend on the steepness of the external gradient. This process requires positive feedback to amplify subtle signalling asymmetries [3] and long-range inhibition to generate a dominant leading edge [4].

Actin polymerization is not only an output of the chemotaxis cascade but also participates in positive and negative feedback interactions with upstream signals. For example, changes in actin polymerization block sustained PI3K lipid products polarity in response to uniform chemoattractant in neutrophils [5], and actin polymerization is essential for recycling the membrane-bound pool of WAVE complex, which itself is a regulator of actin polymerization [6–8]. Most studies

probing the role of the actin cytoskeleton in cell signalling have used actin-depolymerizing drugs, which not only block new assembly but also dramatically alter the existing cytoskeleton and disrupt cell morphology [9–11]. Stabilization of the actin polymer with jasplakinolide leads to hyper-accumulation of the polymer and also results in dramatic alterations to the actin cytoskeleton [12]. Even dual inhibitors similarly fail to arrest actin rearrangements in cells with rapid actin dynamics like neutrophils [12]. Using these tools, it has been difficult to disentangle the many effects of actin on cell signalling.

By using a combination of the pharmacological inhibitors jasplakinolide, latrunculin and Y-27632 (we refer to this cocktail as JLY [12]), we can stabilize the existing actin cytoskeleton while preventing any new rearrangements, thus maintaining cell morphology. JLY potently and rapidly blocks actin depolymerization, polymerization and myosin-induced rearrangements; we hereafter refer to this collection of processes as actin dynamics. Here, we investigated how multiple chemotactic signalling responses (PI3K lipid products, calcium and Pak phosphorylation) are affected by a lack of actin dynamics (JLY treatment) versus a lack of actin polymer (latrunculin treatment) following acute agonist addition (fMLP, formyl-methionyl-leucyl-phenylalanine, and C5a) and during desensitization. We find that stabilized actin polymer extends the period of receptor desensitization following agonist binding and that actin dynamics rapidly reset receptors from this desensitized state.

2. Material and methods

(a) Cell lines and culture

HL-60 cells were cultured as described [7]. Briefly, cells were grown at 37°C, 5% CO_2, in RPMI 1640 media with L-glutamine and 25 mM HEPES (10–041-CM, Mediatech), with 10% heat-inactivated fetal bovine serum (FBS). Cell differentiation was initiated by adding 1.5% DMSO (endotoxin-free, hybridoma-tested; D2650, Sigma) to cells in media. Cells for all experiments were used at 5–6 days after differentiation. For the micropipette experiments, HL-60 cells expressing PH-AKT-GFP were used [3].

(b) Drug treatments

For JLY treatment for all microscopy experiments (figures 1 and 2; electronic supplementary material, movies S6 and S7), cells were treated as described [12], except that the final concentration of latrunculin B was reduced from 5 to 2.5 µM. For latrunculin B (428020, EMD Chemicals) treatment for microscopy experiments, cells were treated as described [12], except that Y-27632 (688001, EMD Chemicals) and jasplakinolide (420127, EMD Chemicals) were not added to the media, and the final concentration of latrunculin B was reduced from 5 to 2.5 µM. Untreated cells were prepared in the same manner, except jasplakinolide, Y-27632, and latrunculin B were not added to the media.

For JLY treatment for non-microscopy-based experiments, inhibitors were added to cells in suspension using a slightly modified version of the protocol. Cells were incubated for 10 min at 37°C, 5% CO_2, in their culture media plus 10 µM Y-27632. After 10 min, cells were gently resuspended by flicking, and an equal volume of 16 µM jasplakinolide, 5 µM latrunculin B and 10 µM Y-27632 (also in culture media) was added. Cells were placed on an end-over-end rotator for 10 min prior to experiments. For latrunculin treatment for non-microscopy-based experiments, the same protocol was used, except that jasplakinolide and Y-27632 were not added to the media. Untreated cells for non-microscopy-based experiments followed the same protocol, except jasplakinolide, Y-27632, and latrunculin B were not added to the media.

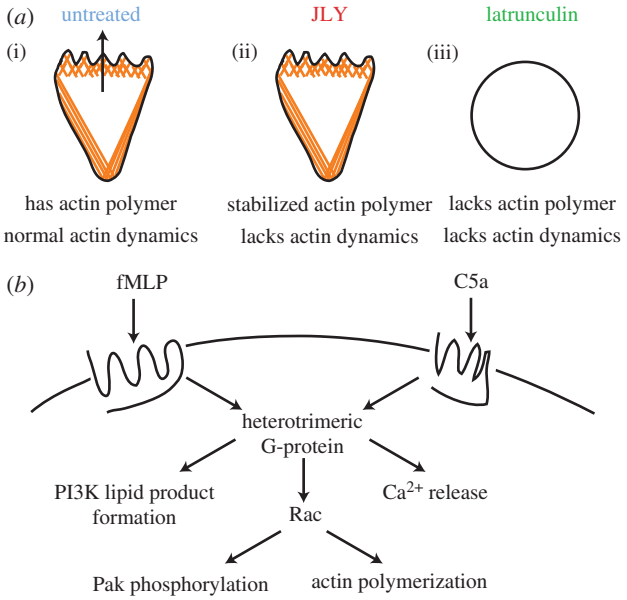

Figure 1. Assessing the impact of actin-targeting pharmacological perturbations on chemotactic signalling. (*a*) Schematic showing differences in actin cytoskeleton between (i) untreated cells, and (ii) JLY-treated or (iii) latrunculin-treated cells. (iii) Latrunculin treatment inhibits actin polymerization, resulting in cells that lack actin polymer and consequently also lack actin dynamics. (ii) JLY treatment inhibits actin polymerization, depolymerization and myosin-based rearrangements, which blocks actin dynamics and consequently freezes the existing actin cytoskeleton. Comparison of JLY- and latrunculin-treated cells allows us to test the role of stabilized actin polymer in signalling, whereas comparison of JLY and untreated cells allows us to test the role of actin dynamics in signalling. (*b*) fMLP and C5a activate two different Gi-linked G-protein coupled receptors (GPCRs) that drive chemotactic signalling. In this work, we draw conclusions about the role of actin in chemotactic signalling by examining differences in PI3K lipid product generation, Pak phosphorylation and calcium release for the three conditions shown in (*a*). (Online version in colour.)

(c) Micropipette assays

Glass capillaries were pulled as described [7] except that they were pulled on a Sutter Model P-97 instead of P-87 (exact program varies based on heating filament properties). Needles were backfilled with a sterile-filtered solution (0.2 µm pore size) containing 1 µM fMLP (F3506, Sigma) and 1 µM Alexa 594 sodium hydrazide (A-10438, Invitrogen) and held by a micromanipulator (MM-89, Narishige). Agonist flow rate from the pipette was controlled as described [7].

(d) Fibronectin coating of glass coverslips

This was performed as described [13], except using 0.005 mg ml^{-1} instead of 0.2 mg ml^{-1} fibronectin to avoid overadhesion of the cells.

(e) Poly-D-lysine coating of clear bottom 96-well plates

Poly-D-lysine hydrobromide (Sigma, P6407) was dissolved at 200 µg ml^{-1} in water and kept at 4°C when not in use. A 70 µl of this solution was added to each well of a 96-well plate, and the solution was allowed to adsorb for 3 h. The wells were then washed 5× with Milli-Q water, and the plate was stored dry at room temperature (23°C) until use.

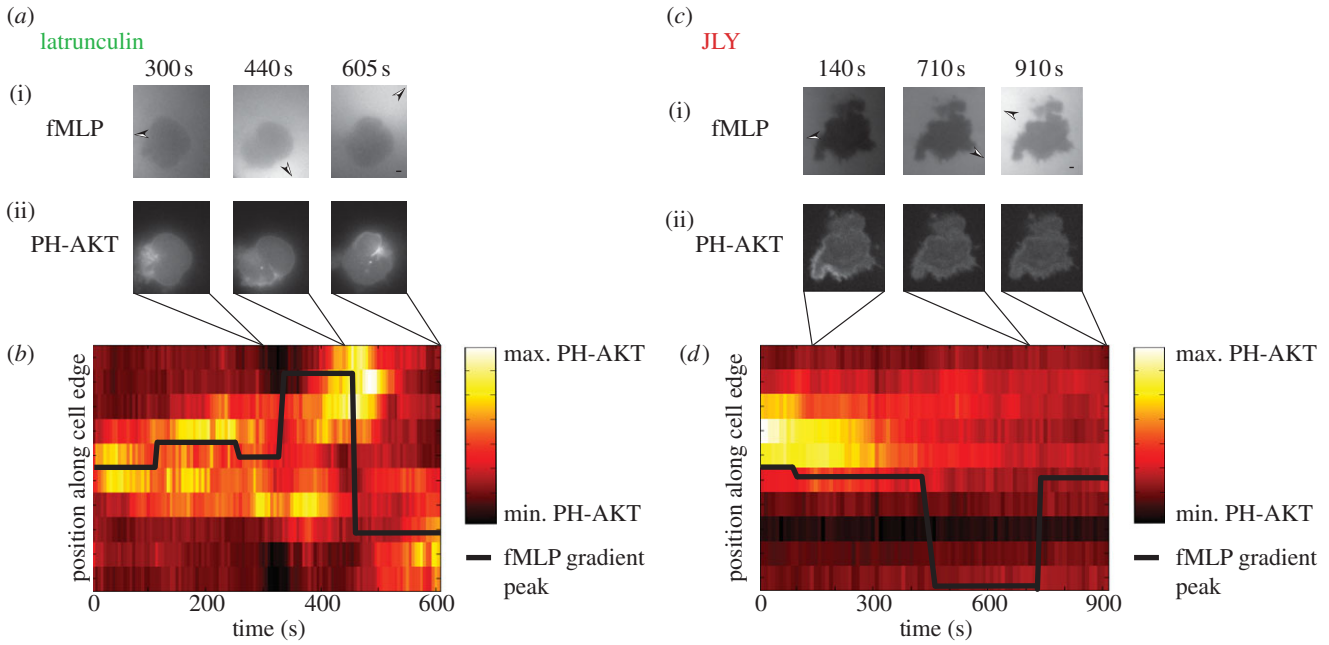

Figure 2. JLY-treated cells fail to persistently sustain PI3K lipid product accumulation in response to a moving agonist gradient. Latrunculin-treated (2.5 µM) cells (*a*, corresponds to the electronic supplementary material, movie S2) or JLY- (2.5 µM latrunculin, 8 µM jasplakinolide and 10 µM Y-27632) treated cells (*c*, corresponds to the electronic supplementary material, movie S3) are presented with a moving micropipette containing 1 µM fMLP agonist and a tracer dye to visualize the agonist gradient. Selected panels show the agonist gradient (*a*(i) and *c*(i)) and the cell's PI3K lipid product response (visualized by PH-AKT-GFP translocation to the plasma membrane; *a*(ii) and *c*(ii)) at three time points. Arrowheads (*a*(i) and *c*(ii)) indicate the direction of the gradient, and scale bars in the lower right corner of the last time point displayed represents 1 µm. (*a*) Latrunculin-treated cells align PI3K lipid product accumulation in the direction of the external gradient for all positions of the pipette. (*c*) By contrast, JLY-treated cells orient PI3K lipid product accumulation in the direction of the external gradient for only the first pipette position and fail to respond to subsequent pipette positions. (*b*,*d*) Heatmaps corresponding to the cells in (*a*) and (*c*) show kymographs of the PI3K lipid product response along the cell periphery. Each column represents a single time point, and each row represents an angular section (sector) of the cell edge. For each time point/sector, light colours correspond to high PI3K lipid product accumulation in that region, whereas darker colours indicate low PI3K lipid product accumulation. A photobleaching correction was applied to each frame of the movie. The overlaid black line indicates the position along the cell edge exposed to the highest concentration of chemoattractant. (Online version in colour.)

(f) Microscopy-based experiments

(i) PI3K lipid product measurements

PH-AKT-GFP-expressing HL-60 cells were plated for 10 min at 37°C, 5% CO_2 on glass coverslips (Lab-Tek, no. 1.5) coated with fibronectin. Cells were drug treated and responses to a micropipette containing fMLP were measured. Images were taken at room temperature (23°C) on a Nikon Eclipse Ti inverted microscope, using a 60× PlanApo TIRF 1.49 NA objective. The light path was modified to contain a confocal scanning head (Solamere Technology group, Yokogawa CSU22). Samples were excited using 488 and 561 nm lasers (Spectral Applied Research, LMM5). Images were recorded using an EM-CCD camera (Photometrics, Evolve 512). Sample drift was minimized using the built-in autofocusing system. NIS Elements 3.2 was used for device control and image acquisition. Still frames shown here were adjusted linearly in ImageJ to enhance contrast. Frames were acquired every 5 s, except for the JLY reorientation experiment (figure 1*c*,*d*), where frames were acquired every 10 s. Typical exposure settings were 33% laser power, 200 ms exposure, Multiplier 264 for the 488 nM channel, and 100% laser power, 400 ms exposure, no multiplier for the 561 channel.

(ii) Calcium scope measurements

Cells were loaded with Fluo-4 AM dye as described for the Flexstation calcium experiments and then either untreated or JLY treated according to the 'Drug treatments' section for microscopy experiments. After 10 min of drug treatment/no treatment, cells were exposed to 1 µM fMLP agonist for 20 min, washed 3× with buffer and left on the slide for 30 min prior to restimulation with 100 nM fMLP. For this secondary addition of agonist, calcium responses were simultaneously observed on the microscope. In the case of the JLY-treated cells, a saturating dose of C5a was added 2 min after addition of 100 nM fMLP. Images were taken at room temperature (23°C) on a Nikon Eclipse TE-2000E inverted microscope, with a 20× Plan Fluor Ph1 DLL objective, NA 0.50 (Nikon). Cells were illuminated with 488 nm light emanating from an arc lamp source (Sutter, Lambda LS). ND 8 and ND 2 filters were placed in the light path to avoid spontaneous activation of the calcium dye. Typical exposure settings were 200 ms, Multiplier 3305. Images were acquired every 5 s.

(g) Flexstation calcium assays

Cells were resuspended in their own media at 1 million cells per ml. Fluo-4 AM (F14201, Invitrogen), a calcium indicator dye, was dissolved in DMSO at 1 mM and kept at −20°C when not in use. 1.5 µM Fluo-4 AM was added to the cells, and they were then incubated at 37°C, 5% CO_2 for 30 min. Next, cells were spun out of media containing Fluo-4 AM and resuspended in fresh culture media. Cells were then left untreated or treated with the appropriate drug (see Drug treatments). Following drug treatment, cells were either directly loaded (1-pulse, figure 5) into a black, clear bottom 96-well Costar plate (07–200–565, Fisher) that had been previously coated with poly-D-lysine, or were first prestimulated with a saturating dose of fMLP (1 µM fMLP) for 10 min, spun at 400*g* × 2 min, washed three times with culture media to remove unbound fMLP and placed on an end-over-end rotator for 30 min (2-pulse, figure 6) prior to loading cells in the plate. Cells were loaded in plate wells (5×10^5 cells/well, in a volume of 180 µl). After loading, the plate was spun at 400*g* × 5 min to pellet cells to the bottom at roughly monolayer density. The plate was quickly transferred from the centrifuge to the Flexstation 3 (Molecular Devices),

which had been previously loaded with tips and a compound plate containing the chosen agonist dilutions (either fMLP or C5a (C5788, Sigma)). The following Flexstation settings were used to add agonist and image the calcium dye:

read mode	fluorescence, bottom read
Ex	495 nm
Em	525 nm
auto cut-off	515 nm
readings	10
PMT	medium
timing	70 s
interval	2 s
reads	36
assay plate	96-well Costar blk/clrbtm
compound transfer	
initial volume	80 µl
transfers	1
pipette height	125 µl
volume	60 µl
rate	2
time point	17 s
compound source	Costar 96 Vbtm 0.3 ml
AutoCalibrate:	on
AutoRead:	off

(h) Pak phosphorylation assay

Cells were resuspended to a concentration of 1 million ml^{-1} in culture media, and left untreated or treated with drug (see Drug treatments). After treatment, cells were spun out of culture media and resuspended in the same media lacking FBS, plus 1× drug (if applicable). FBS was left out of the assay buffer because in the later steps it precipitated and interfered with our ability to detect Pak phosphorylation. We stimulated cells with 100 nM fMLP and quenched the reaction by adding aliquots of the cell mixture to ice-cold 20% trichloroacetic acid plus 40 mM sodium fluoride plus 20 mM beta-glycerol phosphate (50020, Fluka) at the indicated time points. Pellets were washed and resuspended in Laemmli protein sample buffer (161–0737, BioRad) containing 5% β-mercapto-ethanol. Protein bands were separated by gel electrophoresis on a Novex 4–12% Bis–Tris SDS-PAGE gel (NP0323BOX, Invitrogen) and transferred to nitrocellulose using a semi-dry transfer apparatus. The blot was first incubated with a 1 : 1000 dilution of both rabbit anti-phosphoPAK (2605, Cell Signaling, which recognizes Phospho-PAK1 (Ser199/204)/PAK2 (Ser192/197)) and mouse anti-Rac1(610651, BD Biosciences; used as a loading control). The blot was washed and incubated with the fluorescent secondary antibodies AlexaFluor 680 Donkey-anti-Rabbit and AlexaFluor 800 Donkey-anti-Mouse, and protein bands were imaged using Odyssey Infrared Imaging System (Li-COR, Biosciences).

(i) Data analysis

For micropipette data, cell boundaries were defined manually in ImageJ. Custom scripts using the Matlab image processing toolbox were written to define cell edge, and heatmaps showing PI3K lipid product intensity across the cell edge were generated as described [7]. Position of micropipette was also calculated as described [7]. For calcium assays, raw data was preprocessed in SoftMax Pro v. 5.4 (as described in the electronic supplementary material, figure S1) and transferred to an Excel spreadsheet for plotting.

For Pak phosphorylation assays, protein levels were quantified after background subtraction in ImageJ. Pak phosphorylation responses were normalized to the loading control (Rac1). Statistical tests (paired Student's *t*-tests, $p < 0.05$) to verify whether two distributions were significantly different were performed in Matlab v. 7.4.

3. Results

In this work, we set out to determine the role of actin dynamics in regulating signalling responses downstream of chemoattractant in neutrophils. Differentiated, neutrophil-like HL-60 cells were either untreated, JLY treated or latrunculin treated (figure 1*a*), and chemotactic responses (PI3K lipid products, Pak phosphorylation and calcium; figure 1*b*) were measured. JLY treatment blocks all actin dynamics (actin polymerization, depolymerization and myosin-based rearrangements; electronic supplementary material, movie S1), whereas latrunculin treatment only inhibits actin polymerization, which results in disassembly of the existing actin cytoskeleton. By comparing JLY- and latrunculin-treated cells, we were able to examine the effect of stabilized actin polymer on chemotactic responses. By comparing JLY treated and untreated cells, we were able to examine the effect of blocking actin dynamics on chemotactic responses.

(a) Actin dynamics are required for persistent PI3K lipid product accumulation induced by chemotactic gradients

We first used a micropipette assay to investigate the role of actin dynamics in aligning internal signalling cascades with focal agonist gradients (figures 2 and 3). This assay has the benefit of being able to simultaneously assess many facets of chemotaxis—adaptation, polarization, alignment with external signals and ability to reorient to moving cues. We reasoned that this assay could help us broadly identify which aspects of chemotactic signalling depend on actin dynamics.

Changes in cell morphology cannot be used to measure cell response to chemoattractant, because the actin cytoskeleton has been either stabilized using JLY, or depolymerized using latrunculin. Fluorescent PI3K lipid product reporters (such as the PH domain of AKT) have been extensively used to measure responses to chemotactic agonists in immobilized cells [5,14–20]. Previous reports show that latrunculin treatment of *Dictyostelium* and neutrophils does not block the ability of cells to align intracellular gradients of PI3K lipid products with extracellular agonist gradients.

We first tested whether actin dynamics were required for a cell to align internal signalling cascades with moving external gradients (figure 2), an ability that is absolutely essential for neutrophils to chase prey. As previously reported for latrunculin-treated *Dictyostelium* [17,19], latrunculin-treated neutrophils are able to continually reorient PI3K lipid products to align with a moving micropipette (figure 2*a*,*b* and electronic supplementary material, movie S2). JLY-treated cells (figure 2 and electronic supplementary material, movie S3) are initially able to align PI3K lipid products with the external gradient (figure 2*c*,*d*, left) but are unable to do so for subsequent positions of the micropipette (figure 2*c*,*d*, middle and right). As latrunculin-treated cells can continually reorient their internal PI3K lipid product distribution, whereas JLY-treated cells fail

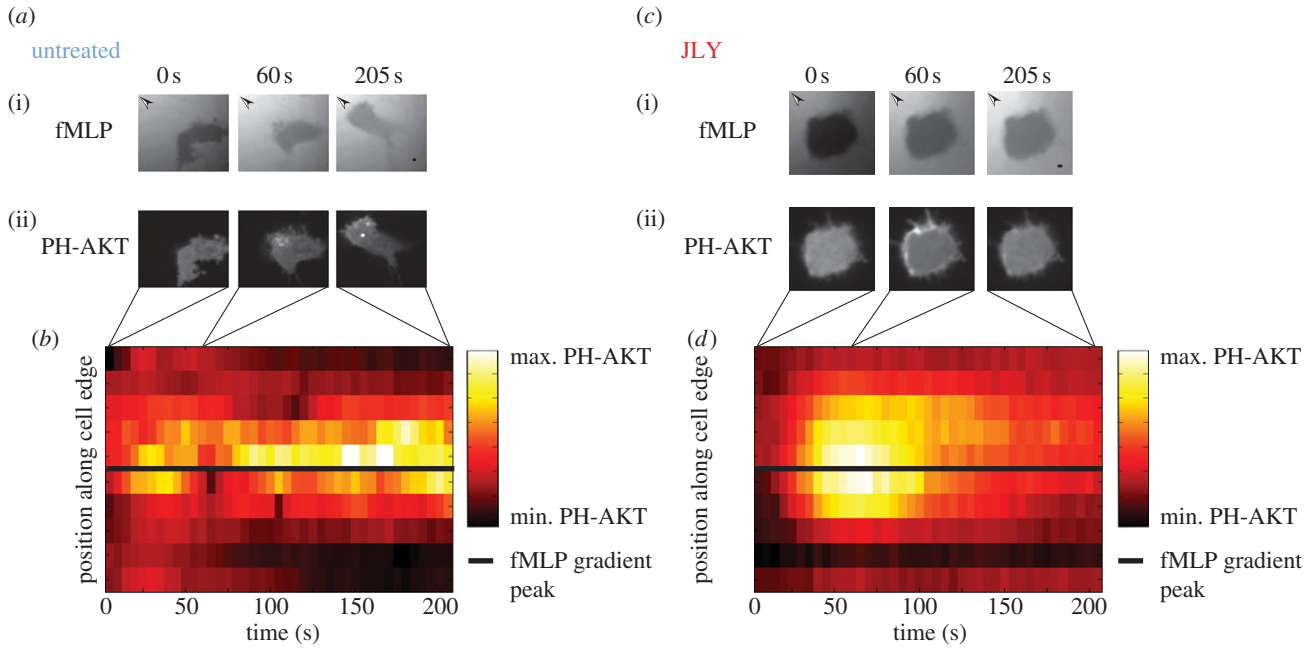

Figure 3. JLY-treated cells fail to persistently sustain PI3K lipid product accumulation in response to a stationary agonist gradient. Untreated (*a*, corresponds to the electronic supplementary material, movie S4) and JLY-treated (*c*, corresponds to the electronic supplementary material, movie S5) cells are presented with a micropipette containing 1 µM fMLP agonist and a tracer dye to visualize the agonist gradient. At $t = 0$ s, the micropipette is moved into close proximity with the cell, where the pipette remains stationary for the remainder of the experiment. Selected panels show the agonist gradient (*a*(i) and *c*(i)) and the cell's PI3K lipid product response (visualized by PH-AKT-GFP translocation to the plasma membrane; *a*(ii) and *c*(ii)) at three time points. Arrowheads (*a*(i) and *c*(i)) indicate the direction of the gradient, and scale bars in the lower right corner of the last time point displayed represents 1 µm. (*a*) Untreated cells respond with PI3K lipid products oriented in the direction of the external gradient at 60 s (*a*, middle panels) and 205 s (*a*, right panels). (*c*) JLY-treated cells orient PI3K lipid products in the direction of the external gradient at 60 s (*c*, middle panels) but not at 205 s (*c*, right panels), indicating an inability to sustain PI3K lipid product accumulation at later times following agonist exposure. (*b*,*d*) Heatmaps corresponding to the cells in (*a*) and (*c*) show the kymograph of PI3K lipid product response along the cell periphery, as in figure 2. (Online version in colour.)

to do so, our results indicate that stabilized actin polymer prevents cells from reorienting PI3K lipid products.

The observed defect in JLY-treated cells could be owing to an inability to respond to moving gradients, or it could be owing to an inability to respond to any gradient at later times following agonist exposure. To discriminate between these possibilities, we tested whether blocking actin dynamics prevented cells from persistently aligning internal signalling cascades with a stationary external gradient (figure 3). PH-AKT-GFP-expressing cells were either left untreated (figure 3*a*,*b* and electronic supplementary material, movie S4) or JLY treated (figure 3*c*,*d* and electronic supplementary material, movie S5), and a micropipette was moved into close proximity with cells at $t = 0$. As expected, untreated cells can persistently align intracellular PI3K lipid products with the external gradient (figure 3*a*,*b*, centre and right). Importantly, when measured using a bulk assay, PI3K lipid product activity undergoes adaptation on a time scale roughly consistent with that of other chemotactic responses [21]. The persistent pool of PI3K lipid products that can be visualized here represents only a small fraction of the total amount of PI3K products generated. At early times (60 s) after exposure to the micropipette, JLY-treated cells were also able to align intracellular PI3K lipid products with the external gradient (figure 3*c*,*d*, centre). However, the PI3K lipid product enrichment on the plasma membrane faded over time and was completely abolished by 205 s (figure 3*c*,*d*, right) for JLY-treated cells. This defect is not observed in cells that simply lack actin polymer; latrunculin-treated *Dictyostelium* can persistently maintain PI3K lipid products in response to agonist gradients [18,20]. We conclude that for cells with an actin cytoskeleton, actin dynamics are required to sustain PI3K lipid product polarity in response to external gradients.

(b) Actin dynamics are required for persistent Pak phosphorylation downstream of uniform agonist

The persistence defects for JLY-treated cells in the micropipette assay could reflect a particular issue with gradient interpretation or could reflect a more general inability of JLY-treated cells to respond to agonist during later phases of agonist exposure. To discriminate between these possibilities, we moved to a simpler agonist presentation (uniform instead of gradient) and used a population-level readout to more quantitatively measure the extent of the defect. For this purpose, we used Western blotting of stimulated cells to assay Pak phosphorylation, which is triggered downstream of activated Rac [22–24] (figure 4*a*). While PI3K is known to have a context-dependent role in neutrophil polarity and chemotaxis [25], Rac is essential for chemotaxis in these cells [26,27]. None of the pharmacological manipulations inhibited the initial peak response of Pak phosphorylation that follows chemotactic stimulation at the 30 s time point. However, Pak phosphorylation levels drop significantly from 30 to 60 s in JLY-treated cells, while remaining steady in both untreated and latrunculin-treated cells (figure 4*a*). This difference was determined to be statistically significant for $n = 4$ independent runs ($p < 0.05$, paired Student's *t*-test, figure 4*b*). The differences between the latrunculin- and JLY-treated cells show that stabilized actin polymer prevents sustained Pak phosphorylation responses at 1 min after agonist exposure. As untreated cells also show a more sustained response than JLY cells, we further conclude that for cells with an existing actin cytoskeleton, actin

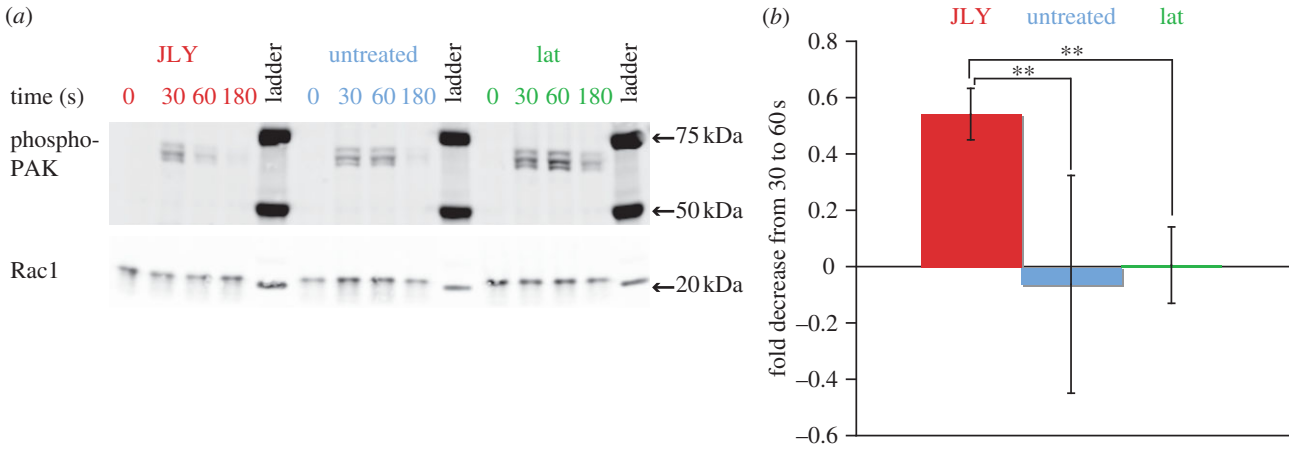

Figure 4. Pak phosphorylation in JLY-treated cells decays more rapidly than in untreated or latrunculin-treated cells. (*a*) Western blot measuring Pak phosphorylation in JLY, untreated or latrunculin-treated cells at different times following uniform addition of 100 nM fMLP agonist. JLY-treated cells respond in a more transient fashion than do untreated or latrunculin-treated cells, with a large decrease in signalling occurring between the 30 and 60 s time points. (*b*) Quantification of the fold decrease from the 30 s to the 60 s time point for $n = 4$ independent runs of the experiment shown in (*a*). Each run was taken on a different day from a different flask of cells. Each Pak phosphorylation measurement was normalized to its loading control (Rac1). A statistically significant decrease was seen in JLY cells compared with either untreated or latrunculin-treated cells ($p < 0.05$, paired Student's *t*-test). (Online version in colour.)

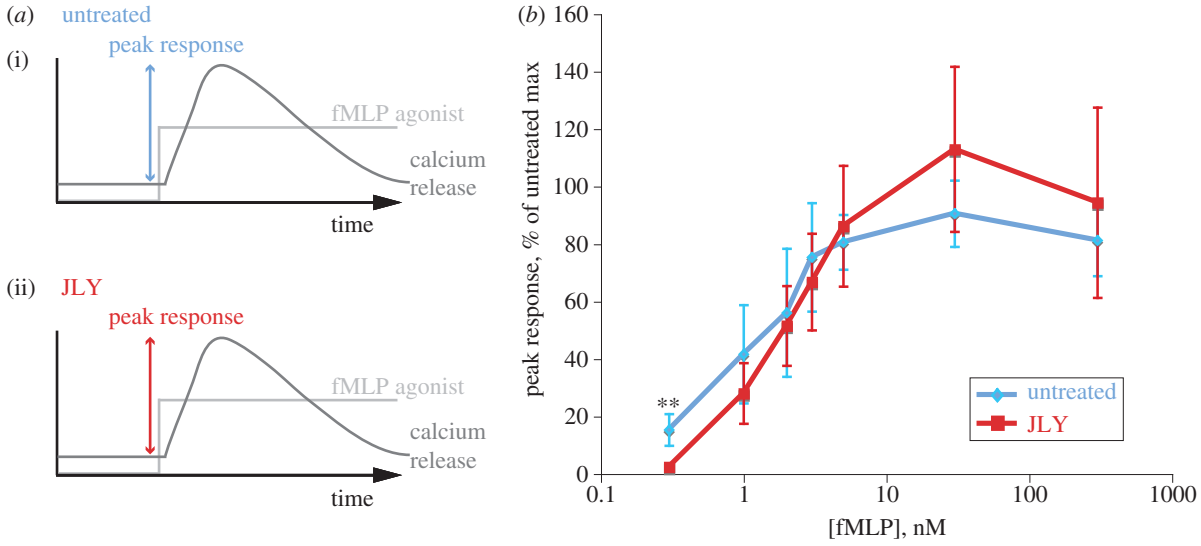

Figure 5. Initial calcium response is largely unaffected by JLY treatment. (*a*) Schematic showing the set-up and results for the experiment performed in (*b*). Cells are split into two groups: (i) untreated or (ii) JLY-treated. Cells are spun in a 96-well plate, and uniform agonist is added to the cells. Calcium release is simultaneously measured, and the difference between the peak and the baseline is reported as the response. (*b*) Calcium responses were measured for JLY and untreated cells, spanning three orders of magnitude of fMLP agonist concentrations. The plots show means and error bars (width of error bars denotes 2 × s.e.m.) for data from $n = 5$ independent paired runs for JLY and untreated cells. Each run was taken on a different day from a different flask of cells. Only at the very lowest dose (0.3 nM) was a statistically significant difference (double asterisks, $p < 0.05$, paired Student's *t*-test) observed for JLY-treated cells; we suggest that actin dynamics may play a role in amplifying responses to threshold doses of agonist. For all other chemoattractant concentrations assayed (1–300 nM fMLP), there was not a statistically significant difference between the untreated and JLY-treated cells. (Online version in colour.)

dynamics permit sustained Pak phosphorylation responses at 1 min after agonist exposure.

(c) Role of actin dynamics in chemoattractant receptor desensitization/resensitization

To restrict potential mechanisms by which actin dynamics might affect responses to agonist, we investigated the question of when JLY-treated cells first become diminished in their agonist response. We sought to use a quantitative, live readout of cell response that would allow us to examine the timing of the defect more carefully. For this purpose, we analysed the increase in cytosolic calcium levels that is triggered downstream of chemotactic stimulation. Using the FlexStation 3 plate reader, we can simultaneously add agonist to cells while measuring fluorescence intensity changes in the cell-permeable calcium indicator Fluo-4AM. Following agonist addition, cytosolic calcium levels peak rapidly (5–10 s for a saturating dose of fMLP), making the peak response a good measure of the initial cellular response to agonist. Peak calcium response values were calculated from kinetic traces as described (see electronic supplementary material, figure S1).

We added different concentrations of uniform fMLP agonist to cells that were either untreated (figure 5*a*(i)) or JLY treated (figure 5*a*(ii)) in order to calculate dose-response curves for each condition (figure 5*b*). This was repeated

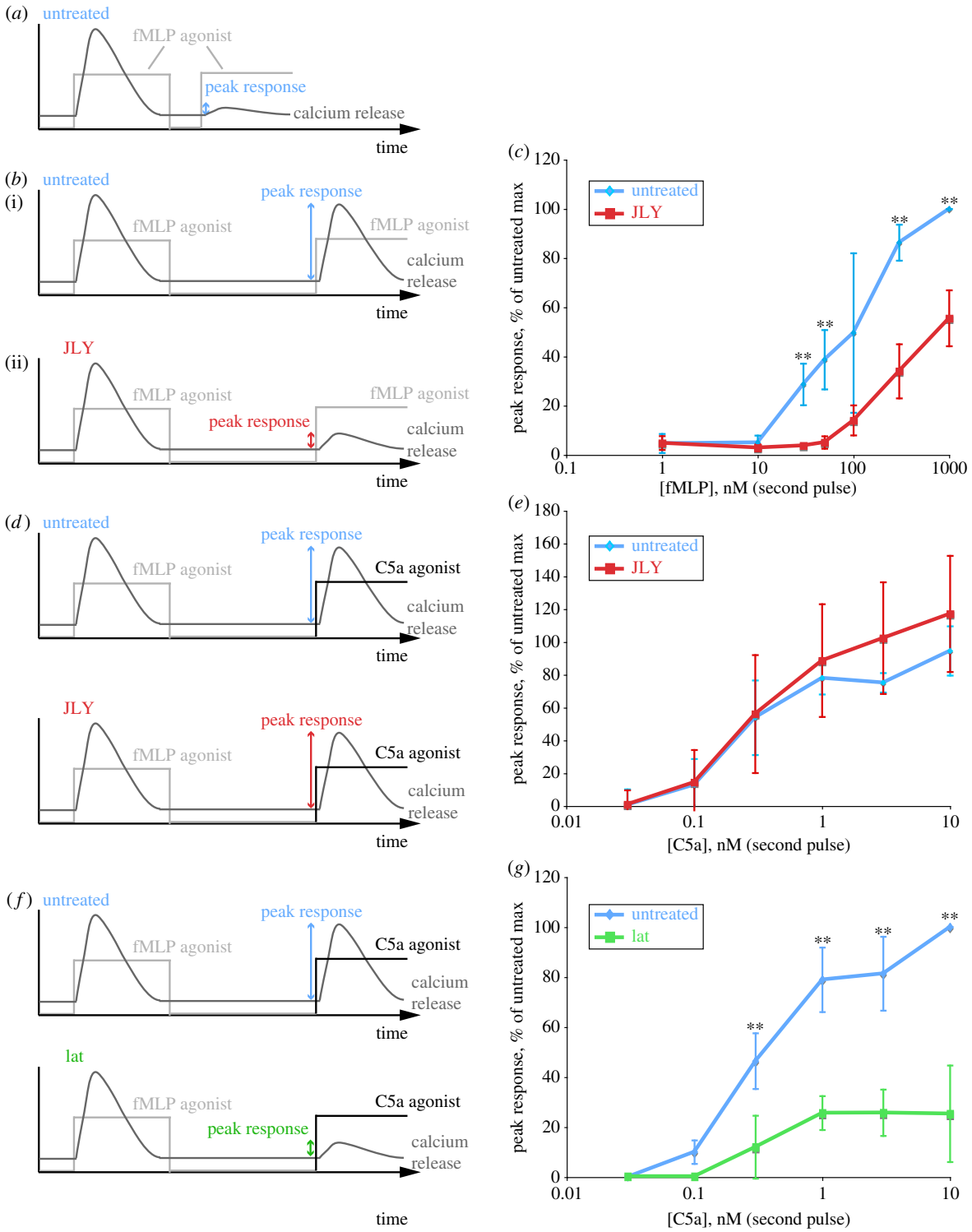

Figure 6. JLY-treated cells exhibit prolonged homologous desensitization of chemoattractant receptors. (*a*) Schematic showing calcium release if two agonist pulses are given in short succession to untreated cells. Without sufficient time to recover from the adapted state, the cell will not be able to respond effectively to the second pulse. (*b*) Schematic showing the set-up and results for the experiment performed in (*c*). The set-up follows the schematic shown in figure 5*a*, where cells are split into untreated or JLY-treated groups, and uniform fMLP agonist is added. After a first round of stimulation, cells are washed three times with buffer to remove agonist and left in wash buffer for 40 min before a second addition of uniform fMLP agonist. Unlike the response in figure 6*a*, the 40 min wash step gives sufficient time for untreated cells to respond effectively to the second pulse. Following the methods described in figure 5*a*, the calcium response to this second pulse is measured and plotted in (*c*). (*c*) Dose-response curve for the second fMLP agonist addition for JLY and untreated cells, showing means and error bars (width of error bars denotes 2 $\times$ s.e.m.) for $n = 3$ independent runs. JLY-treated cells had significantly lower response than untreated cells across a wide range of concentrations (double asterisks, $p < 0.05$, paired Student's *t*-test). (*d*) Schematic showing the set-up and results for the experiment performed in (*e*). This experiment follows the same set-up as for (*b*), except that the second agonist addition differs from the first (C5a, rather than fMLP) and activates a different GPCR. (*e*) Dose-response curve for the C5a agonist addition (following fMLP pre-treatment) for JLY and untreated cells, showing means and error bars for $n = 3$ independent runs. Under these conditions, JLY-treated cells do not differ from untreated cells in their response. (*f*) Schematic showing the set-up and results for the experiment performed in (*g*). This experiment follows the set-up in (*d*), except that cells are treated with latrunculin instead of JLY. (*g*) Dose-response curve for the C5a agonist addition (following fMLP pre-treatment) for latrunculin versus untreated cells, showing means and error bars for $n = 3$ independent runs. Latrunculin-treated cells are significantly weakened in their ability to mobilize calcium in response to C5a after desensitization with fMLP. The difference between untreated and latrunculin-treated cells' response is statistically significant ($p < 0.05$, paired Student's *t*-test) across a wide range of agonist concentrations (0.3–10 nM C5a). (Online version in colour.)

for $n = 5$ independent experiments, measured using cells from different flasks on different days. We plotted the peak responses as a per cent of the maximum response from untreated cells across all concentrations for that run (figure 5*b*). We observed a slight delay in the amount of time needed to reach the peak for JLY-treated cells relative to untreated cells (see electronic supplementary material, figure S2), but for almost all of the concentrations measured, the peak calcium responses of JLY-treated and untreated cells were similar. The lone difference in agonist sensitivity was at the lowest responding dose for untreated cells (0.3 nM fMLP), where a statistically significant difference ($p < 0.05$, paired Student's *t*-test) between untreated and JLY-treated cells was found. Our data suggest that there may be a role for actin dynamics in amplifying responses to threshold levels of fMLP agonist. However, for most concentrations of fMLP agonist, our data show that blocking actin dynamics does not have a significant effect on the initial calcium response.

Given that JLY-treated cells are unaffected in their initial calcium response to agonist, why might they be unable to respond properly to agonist at later times? Most chemotactic responses, including calcium, adapt shortly after exposure to an acute increase in agonist—that is, they reach a peak and rapidly return to equilibrium near their pre-agonist exposure levels. This adjustment of cellular sensitivity allows cells to detect relative changes rather than steady-state concentrations of ligand. This ability is thought to enable cells to chemotax properly over more than four orders of magnitude of agonist concentrations [1,2]. We hypothesized that improper desensitization/resensitization following agonist exposure might diminish the responsiveness and persistence of JLY-treated cells.

To investigate the role of the actin cytoskeleton in receptor desensitization, we used a classic assay of neutrophil desensitization. Cells exposed to a large concentration of fMLP lose their ability to respond to the same agonist if re-stimulated at short times after the first pulse (figure 6*a*, [2,28,29]) but regain their ability to respond to fMLP at later times once sensitivity is reset (figure 6*b*(i), [30]). Cells, untreated or pre-treated with JLY, were exposed to a pulse of fMLP agonist to trigger adaptation. Agonist was then washed away, and cells remained in agonist-free buffer for 40 min, long enough to allow sensitivity to be reset in control cells. A second pulse of fMLP agonist was then delivered, and the responses of untreated (figure 6*b*(i)) versus JLY-treated cells (figure 6*b*(ii)) were measured. This response to the second pulse of agonist allowed us to measure changes in agonist sensitivity caused by the first pulse of agonist. While calcium signalling is not a direct readout of receptor activity, termination of receptor signalling leads to rapid termination of all downstream chemotaxis signalling responses [31], indicating that a loss of sensitivity at the receptor level should result in diminished downstream signalling.

First, to assay desensitization, we investigated whether actin dynamics affected cell sensitivity upon subsequent re-exposure to the same agonist. We found that JLY-treated cells were much less sensitive than untreated cells upon re-exposure to fMLP (figure 6*c*). Importantly, this effect was not simply owing to a gradual degradation of cell responsiveness caused by prolonged JLY treatment, because cells had normal acute calcium response even following 1 h of JLY incubation (see electronic supplementary material, figure S3). We saw statistically significant differences ($n = 3$ independent runs) for almost all concentrations where untreated cells showed any calcium response. The one dose assayed where we did not see a statistically significant difference was at 100 nM fMLP, potentially owing to its position around the EC50 (half maximal effective concentration) of the curve where cell responses were the most variable between runs. There was also a large shift in overall sensitivity between the curves—about a sevenfold difference in sensitivity over a 20-fold range of agonist concentrations (50 nM to 1 µM fMLP). Similar results were seen for homologous desensitization using C5a instead of fMLP (see electronic supplementary material, figure S4). We conclude that blocking actin dynamics extends the period of desensitization following agonist exposure.

The mechanism(s) by which cells adapt to chemotactic agonist are poorly understood [32]. We were interested in identifying which level(s) of the chemotactic cascade displayed prolonged desensitization when actin dynamics were blocked. Towards this end, we sought to activate cytoplasmic calcium increases by some other means than fMLP stimulation for the second pulse. By activating the same response through an alternate pathway, we hoped to pinpoint the level of the cascade at which desensitization acts. We repeated the pulse-wash-pulse experiments from figure 6*b*, but using C5a instead of fMLP for the second pulse (figure 6*d*). The pathway of C5a activation of calcium differs from fMLP only at the receptor level, where it activates a different Gi-linked GPCR [33]. Following receptor activation, both pathways activate a common set of downstream effectors to trigger increases in cytoplasmic calcium levels. Prestimulation with fMLP did not have an effect on the relative sensitivity of JLY-treated and untreated cells to C5a (see electronic supplementary material, figure S5), justifying the use of C5a as an orthogonal input to fMLP for activating calcium responses.

By contrast to the reduced sensitivity of JLY-treated cells when fMLP was used for the second pulse (figure 6*c*), JLY-treated cells were no less sensitive than untreated cells when C5a was used for the second pulse (figure 6*e*), indicating that the desensitization observed in figure 6*c* was homologous. Similar results matching figure 6*c*,*e* were also seen when the calcium response of individual cells was visualized by fluorescence microscopy (see electronic supplementary material, movies S6 and S7). This result rules out trivial explanations for lack of response in JLY-treated cells, such as depletion of calcium stores or complete lack of cell response at later times following drug treatment. Unlike JLY cells, latrunculin-treated cells are unable to respond effectively to C5a agonist after desensitization with fMLP (figure 6*f*,*g*). These data suggest that at least for calcium signalling, prolonged JLY treatment does not cause cells to be sick, whereas prolonged latrunculin treatment does. Satisfyingly, a rationally optimized combination of actin inhibitors appears to make cells less sick than individual inhibitors, consistent with the ability of JLY, but not individual inhibitors, to maintain the structure of the existing cytoskeleton. Taken together, our data suggest that the portion of the adaptation machinery that depends on actin dynamics acts in an agonist-dependent, receptor-specific fashion.

4. Discussion

In this work, we used a pharmacological cocktail that inhibits actin polymerization, depolymerization and myosin-based rearrangements to investigate the role of actin dynamics in shaping chemotactic signalling responses. Our approach

complements and extends previous studies that have primarily relied on drugs that completely depolymerize or change the organization of the existing actin cytoskeleton. Our experiments show a lack of persistence in chemotactic signalling for cells with a stabilized actin cytoskeleton. JLY-treated cells are unable to maintain PI3K lipid product polarization in response to external gradients (figures 2 and 3), and Pak phosphorylation decays more rapidly in JLY-treated cells (figure 4). This lack of persistence is not observed for latrunculin-treated cells (figures 2 and 4), indicating that the defect is owing to stabilized actin polymer, as opposed to a lack of new polymerization. JLY-treated cells have a similar calcium response as untreated cells upon initial exposure to chemoattractant (figure 5*a*,*b*). However, when presented with successive pulses of the same agonist (fMLP), JLY-treated cells exhibit a weaker calcium response than untreated cells (figure 6*a*,*b*), indicating that actin dynamics enhance recovery from the adapted state that follows agonist binding. JLY-treated cells exhibit the same sensitivity as untreated cells when exposed to an agonist (C5a) that targets a different Gi-linked GPCR for the second pulse (figure 6*c*,*d*), indicating that the JLY-potentiated desensitization is receptor-specific. Our results suggest that stabilized actin polymer extends the period of receptor desensitization that follows agonist binding and that actin dynamics enhance the recovery of receptors from this adapted state.

Previous studies have suggested that following agonist binding to a chemoattractant receptor, interactions between the receptor and the actin cytoskeleton may promote receptor desensitization. Several seconds after agonist addition, agonist-bound receptors both rapidly desensitize [31] and form complexes with the actin cytoskeleton [34–37]. Furthermore, cytochalasin treatment, which depolymerizes the actin cytoskeleton, has been shown to alleviate desensitization of some downstream responses, for example superoxide signalling [38]. Intriguingly, desensitization of other downstream responses such as calcium signalling [38] and PI3K lipid product accumulation (see electronic supplementary material, figure S6) are not alleviated by actin depolymerization, suggesting either that actin polymer acts at the level of the receptor but is only essential for desensitization of a subset of chemotactic effectors, that actin polymer acts to desensitize chemotactic responses below the level of receptor, or that complete depolymerization of the actin cytoskeleton could be detrimental to some signalling pathways [39,40] (figure 6*g*). It is difficult to discriminate between these possibilities using only global actin depolymerization.

Here, we test whether stabilizing actin polymer with JLY is sufficient to modulate receptor desensitization, as opposed to testing whether actin depolymerization triggers receptor resensitization through use of cytochalasin or latrunculin alone. Here, we show that JLY-treated cells exhibit potentiated desensitization at the level of the receptor (figure 6). Consistent with work showing that all measured chemotactic signalling responses terminate rapidly after receptor signalling is blocked [31], we show that PI3K lipid product generation (figures 2 and 3) and Pak activation (figure 4) terminate more quickly in JLY-treated cells. These observations suggest that stable actin polymer suffices to enhance receptor desensitization and that early shutoff is likely to be observed in most, if not all, downstream chemotactic responses.

How do we reconcile our observations that stable actin polymer suffices to extend the duration of receptor desensitization for multiple effector pathways with previous studies showing that actin depolymerization only reactivates a subset of signalling pathways? The simplest explanation is that interaction with actin polymer is not the sole mode of receptor desensitization. Other modes of receptor desensitization, for instance receptor phosphorylation, are known to participate in the adaptation process. Formyl peptide receptor phosphorylation has been shown to be both necessary (in transfected U937 cells, [29]) and sufficient (in solubilized membranes, [41,42]) for persistent receptor desensitization. Adaptation of multiple chemotactic responses occur in an actin-independent fashion [5,16,43,44]. Furthermore, some modes of receptor resensitization, for instance exposure to platelet activating factor (PAF), results in formyl peptide receptor reactivation even in the absence of actin polymer [45]. As different chemotactic responses may have different requirements in terms of the receptor state needed to trigger them [46], removal of actin polymer via drug treatment may not be sufficient to cause reactivation of all downstream chemotactic responses.

Taken together, these data suggest that actin polymer, receptor phosphorylation and the as-of-yet unidentified mechanism for PAF-based resensitization represent independent, possibly interacting modes of controlling receptor activity. Actin could serve to modulate the phosphorylation state of the receptor, perhaps by preventing phosphatase access to the receptor. Another potential mechanism is one in which inactive receptors bound to the actin cytoskeleton are compartmentalized in a separate microdomain within the plasma membrane where they are unable to interact with G-protein [36,37]. JLY treatment provides a way of trapping the actin-modulated desensitized state and could facilitate future mechanistic interrogation of how actin regulates receptor desensitization and resensitization.

We propose that disruption of receptor–actin cytoskeleton complexes, either owing to actin dynamics in untreated cells or destruction of the cytoskeleton in latrunculin-treated cells, permits rapid receptor resensitization. No appreciable endocytosis of the formyl peptide receptor occurs in HL-60 cells at 1 min following agonist exposure [47], making endocytosis followed by recycling too slow to explain the reduced Pak phosphorylation in JLY-treated cells by 1 min (figure 4) or the reduced PI3K lipid product accumulation at 3 min (figure 3). The rapid decay of the Pak phosphorylation (figure 4) and PI3K lipid products generation (figure 3) in JLY-treated cells is also unlikely to be owing to actin's involvement in a positive feedback loop [3,48], because latrunculin-treated cells (which lack actin polymer) do not show the same rapidly decaying responses. A role for actin dynamics in disrupting receptor–actin complexes would be consistent with our data at both short (figures 2–4) and long time scales (figure 6).

Our data also indicate that actin dynamics increase cell sensitivity to threshold doses of agonist. We find a statistically significant decrease in sensitivity for JLY-treated cells at the lowest doses of agonist for both fMLP (figure 5*b*) and C5a (see electronic supplementary material, figure S5). This difference could reflect a lack of actin dynamics leading to increased receptor desensitization, which could tip the scales towards lack of response at threshold doses of agonist.

The methods employed in this paper complement and extend previous means of interrogating the role of actin in signalling. JLY treatment is the only available tool for studying the role of actin dynamics separately from the role of actin polymer. In the context of this work, we have used JLY to

trap a long-lived form of the desensitized receptor, which should aid future studies in determining the mechanism by which actin–receptor interactions promote chemoattractant receptor inactivation. Our methodology and results differ from approaches in which only actin-depolymerizing drugs are used to manipulate the actin cytoskeleton.

Why might it be useful to have actin regulate the activity of the receptor? Actin polymer could act as a homeostat by negative feedback regulation of receptor signalling. This might buffer the overall output of the chemotactic cascade even if levels of intermediate signalling molecules fluctuate significantly. An increase in concentrations of chemotactic signalling intermediates would lead to increased actin polymerization, which would then decrease the sensitivity of the receptor.

It has been known for several decades that different sides of a migrating cell have different sensitivities to agonist. Classic experiments by Zigmond *et al*. [49] show that the front edge of a migrating neutrophil is more sensitive to agonist than the sides and the back. For *Dictyostelium*, the bound chemoattractant agonist dissociates faster from the leading edge than it does from the trailing edge [50], potentially reflecting more rapid resensitization of receptors at the leading edge. These asymmetries parallel the front/back asymmetries of actin polymerization, depolymerization and myosin-induced contraction [51–56]. We propose that spatial differences in actin dynamics could explain the increased agonist sensitivity for the front versus back of polarized cells during chemotaxis.

Acknowledgements. We thank Henry Bourne and members of the Weiner Lab for a critical reading of the manuscript, and Oliver Hoeller for useful conversations about organizing figures. We thank for Tejal Desai, Daniel Fletcher, Wallace Marshall, Henry Bourne and members of the Weiner Lab for helpful discussions about this research.

Funding statement. This work was supported by an Achievement Rewards for College Scientists (ARCS) Scholarship and a National Institutes of Health traineeship (grant no. 5T32EB009383-03) to S.N.D., a California Institute for Regenerative Medicine fellowship (grant no. TG2-01153) to J.S.P., a National Institutes of Health Nanomedicine Development Center grant no. PN2EY016546 (The Cell Propulsion Laboratory, Center for Synthetic Signaling and Motility Systems Engineering) to J.S.P., J.J.O. and W.A.L., and a National Institutes of Health grant (R01 GM084040) to O.D.W.

References

1. Zigmond SH. 1997 Ability of polymorphonuclear leukocytes to orient in gradients of chemotactic factors. *J. Cell Biol.* **75**, 606–616. (doi:10.1083/jcb.75.2.606)
2. Zigmond SH, Sullivan SJ. 1979 Sensory adaptation of leukocytes to chemotactic peptides. *J. Cell Biol.* **82**, 517–527. (doi:10.1083/jcb.82.2.517)
3. Weiner OD, Neilsen PO, Prestwich GD, Kirschner MW, Cantley LC, Bourne HR. 2002 A PtdInsP(3)- and Rho GTPase-mediated positive feedback loop regulates neutrophil polarity. *Nat. Cell Biol.* **4**, 509–513. (doi:10.1038/ncb811)
4. Houk AR, Jilkine A, Mejean CO, Boltyanskiy R, Dufresne ER, Angenent SB, Altschuler SJ, Wu LF, Weiner OD. 2012 Membrane tension maintains cell polarity by confining signals to the leading edge during neutrophil migration. *Cell* **148**, 175–188. (doi:10.1016/j.cell.2011.10.050)
5. Wang F, Herzmark P, Weiner OD, Srinivasan S, Servant G, Bourne HR. 2002 Lipid products of PI(3)Ks maintain persistent cell polarity and directed motility in neutrophils. *Nat. Cell Biol.* **4**, 513–518. (doi:10.1038/ncb810)
6. Weiner OD, Marganski WA, Wu LF, Altschuler SJ, Kirschner MW. 2007 An actin-based wave generator organizes cell motility. *PLoS Biol.* **5**, e221. (doi:10.1371/journal.pbio.0050221)
7. Millius A, Dandekar SN, Houk AR, Weiner OD. 2009 Neutrophils establish rapid and robust WAVE complex polarity in an actin-dependent fashion. *Curr. Biol.* **19**, 253–259. (doi:10.1016/j.cub.2008.12.044)
8. Millius A, Watanabe N, Weiner OD. 2012 Diffusion, capture and recycling of SCAR/WAVE and Arp2/3 complexes observed in cells by single-molecule imaging. *J. Cell Sci.* **125**, 1165–1176. (doi:10.1242/jcs.091157)
9. Spector I, Shochet NR, Kashman Y, Groweiss A. 1983 Latrunculins: novel marine toxins that disrupt microfilament organization in cultured cells. *Science* **219**, 493–495. (doi:10.1126/science.6681676)
10. Coue M, Brenner SL, Spector I, Korn ED. 1987 Inhibition of actin polymerization by latrunculin A. *FEBS Lett.* **213**, 316–318. (doi:10.1016/0014-5793(87)81513-2)
11. Cooper JA. 1987 Effects of cytochalasin and phalloidin on actin. *J. Cell Biol.* **105**, 1473–1478. (doi:10.1083/jcb.105.4.1473)
12. Peng GE, Wilson SR, Weiner OD. 2011 A pharmacological cocktail for arresting actin dynamics in living cells. *Mol. Biol. Cell* **22**, 3986–3994. (doi:10.1091/mbc.E11-04-0379)
13. Millius A, Weiner OD. 2009 Chemotaxis in neutrophil-like HL-60 cells. *Methods Mol. Biol.* **571**, 167–177. (doi:10.1007/978-1-60761-198-1_11)
14. Servant G, Weiner OD, Herzmark P, Balla T, Sedat JW, Bourne HR. 2000 Polarization of chemoattractant receptor signaling during neutrophil chemotaxis. *Science* **287**, 1037–1040. (doi:10.1126/science.287.5455.1037)
15. Parent CA, Blacklock BJ, Froehlich WM, Murphy DB, Devreotes PN. 1998 G protein signaling events are activated at the leading edge of chemotactic cells. *Cell* **95**, 81–91. (doi:10.1016/S0092-8674(00)81784-5)
16. Janetopoulos C, Ma L, Devreotes PN, Iglesias PA. 2004 Chemoattractant-induced phosphatidylinositol 3,4,5-trisphosphate accumulation is spatially amplified and adapts, independent of the actin cytoskeleton. *Proc. Natl Acad. Sci. USA* **101**, 8951–8956. (doi:10.1073/pnas.0402152101)
17. Devreotes P, Janetopoulos C. 2003 Eukaryotic chemotaxis: distinctions between directional sensing and polarization. *J. Biol. Chem.* **278**, 20 445–20 448. (doi:10.1074/jbc.R300010200)
18. Xu X, Meier-Schellersheim M, Jiao X, Nelson LE, Jin T. 2005 Quantitative imaging of single live cells reveals spatiotemporal dynamics of multistep signaling events of chemoattractant gradient sensing in *Dictyostelium*. *Mol. Biol. Cell* **16**, 676–688. (doi:10.1091/mbc.E04-07-0544)
19. Jin T, Zhang N, Long Y, Parent CA, Devreotes PN. 2000 Localization of the G protein βγ complex in living cells during chemotaxis. *Science* **287**, 1034–1036. (doi:10.1126/science.287.5455.1034)
20. Dormann D, Weijer G, Parent CA, Devreotes PN, Weijer CJ. 2002 Visualizing PI3 kinase-mediated cell–cell signaling during *Dictyostelium* development. *Curr. Biol.* **12**, 1178–1188. (doi:10.1016/S0960-9822(02)00950-8)
21. Stephens LR, Hughes KT, Irvine RF. 1991 Pathway of phosphatidylinositol(3,4,5)-trisphosphate synthesis in activated neutrophils. *Nature* **351**, 33–39. (doi:10.1038/351033a0)
22. Martin GA, Bollag G, McCormick F, Abo A. 1995 A novel serine kinase activated by rac1/CDC42Hs-dependent autophosphorylation is related to PAK65 and STE20. *EMBO J.* **14**, 4385.
23. Zhang S, Han J, Sells MA, Chernoff J, Knaus UG, Ulevitch RJ, Bokoch GM. 1995 Rho family GTPases regulate p38 mitogen-activated protein kinase through the downstream mediator Pak1. *J. Biol. Chem.* **270**, 23 934–23 936. (doi:10.1074/jbc.270.41.23934)
24. Bagrodia S, Taylor SJ, Creasy CL, Chernoff J, Cerione RA. 1995 Identification of a mouse p21Cdc42/Rac activated kinase. *J. Biol. Chem.* **270**, 22 731–22 737. (doi:10.1074/jbc.270.39.22731)
25. Ferguson GJ *et al*. 2007 PI(3)Kγ has an important context-dependent role in neutrophil chemokinesis. *Nat. Cell Biol.* **9**, 86–91. (doi:10.1038/ncb1517)

26. Gu Y *et al*. 2003 Hematopoietic cell regulation by Rac1 and Rac2 guanosine triphosphatases. *Science* **302**, 445–449. (doi:10.1126/science.1088485)
27. Sun CX, Downey GP, Zhu F, Koh AL, Thang H, Glogauer M. 2004 Rac1 is the small GTPase responsible for regulating the neutrophil chemotaxis compass. *Blood* **104**, 3758–3765. (doi:10.1182/blood-2004-03-0781)
28. O'Flaherty JT, Kreutzer DL, Showell HJ, Vitkauskas G, Becker EL, Ward PA. 1979 Selective neutrophil desensitization to chemotactic factors. *J. Cell Biol.* **80**, 564–572. (doi:10.1083/jcb.80.3.564)
29. Prossnitz ER. 1997 Desensitization of N-formylpeptide receptor-mediated activation is dependent upon receptor phosphorylation. *J. Biol. Chem.* **272**, 15 213–15 219. (doi:10.1074/jbc.272.24.15213)
30. Model MA, Omann GM. 1998 Experimental approaches for observing homologous desensitisation and their pitfalls. *Pharmacol. Res.* **38**, 41–44. (doi:10.1006/phrs.1998.0330)
31. Sklar LA, Hyslop PA, Oades ZG, Omann GM, Jesaitis AJ, Painter RG, Cochrane CG. 1985 Signal transduction and ligand–receptor dynamics in the human neutrophil. Transient responses and occupancy-response relations at the formyl peptide receptor. *J. Biol. Chem.* **260**, 11 461–11 467.
32. Weiner OD. 2002 Regulation of cell polarity during eukaryotic chemotaxis: the chemotactic compass. *Curr. Opin. Cell Biol.* **14**, 196–202. (doi:10.1016/S0955-0674(02)00310-1)
33. Jiang H, Kuang Y, Wu Y, Smrcka A, Simon MI, Wu D. 1996 Pertussis toxin-sensitive activation of phospholipase C by the C5a and fMet-Leu-Phe receptors. *J. Biol. Chem.* **271**, 13 430–13 434. (doi:10.1074/jbc.271.23.13430)
34. Jesaitis AJ, Naemura JR, Sklar LA, Cochrane CG, Painter RG. 1984 Rapid modulation of N-formyl chemotactic peptide receptors on the surface of human granulocytes: formation of high-affinity ligand–receptor complexes in transient association with cytoskeleton. *J. Cell Biol.* **98**, 1378–1387. (doi:10.1083/jcb.98.4.1378)
35. Jesaitis AJ, Tolley JO, Painter RG, Sklar LA, Cochrane CG. 1985 Membrane–cytoskeleton interactions and the regulation of chemotactic peptide-induced activation of human granulocytes: the effects of dihydrocytochalasin B. *J. Cell. Biochem.* **27**, 241–253. (doi:10.1002/jcb.240270306)
36. Jesaitis AJ, Bokoch GM, Tolley JO, Allen RA. 1988 Lateral segregation of neutrophil chemotactic receptors into actin- and fodrin-rich plasma membrane microdomains depleted in guanyl nucleotide regulatory proteins. *J. Cell Biol.* **107**, 921–928. (doi:10.1083/jcb.107.3.921)
37. Jesaitis AJ, Tolley JO, Bokoch GM, Allen RA. 1989 Regulation of chemoattractant receptor interaction with transducing proteins by organizational control in the plasma membrane of human neutrophils. *J. Cell Biol.* **109**, 2783–2790. (doi:10.1083/jcb.109.6.2783)
38. Bylund J, Bjorstad A, Granfeldt D, Karlsson A, Woschnagg C, Dahlgren C. 2003 Reactivation of formyl peptide receptors triggers the neutrophil NADPH-oxidase but not a transient rise in intracellular calcium. *J. Biol. Chem.* **278**, 30 578–30 586. (doi:10.1074/jbc.M209202200)
39. Bengtsson T, Orselius K, Wettero J. 2006 Role of the actin cytoskeleton during respiratory burst in chemoattractant-stimulated neutrophils. *Cell Biol. Int.* **30**, 154–163. (doi:10.1016/j.cellbi.2005.10.017)
40. Klinker JF *et al*. 1994 Mastoparan may activate GTP hydrolysis by Gi-proteins in HL-60 membranes indirectly through interaction with nucleoside diphosphate kinase. *Biochem. J.* **304**, 377–383.
41. Bennett TA, Foutz TD, Gurevich VV, Sklar LA, Prossnitz ER. 2001 Partial phosphorylation of the N-formyl peptide receptor inhibits G protein association independent of arrestin binding. *J. Biol. Chem.* **276**, 49 195–49 203. (doi:10.1074/jbc.M106414200)
42. Prossnitz ER, Sklar LA. 2006 Modulation of GPCR conformations by ligands, G-proteins, and arrestins. *Ernst Schering Foundation Symp. Proc.* **2**, 211–228.
43. Takeda K, Shao D, Adler M, Charest PG, Loomis WF, Levine H, Groisman A, Rappel WJ, Firtel RA. 2012 Incoherent feedforward control governs adaptation of activated Ras in a eukaryotic chemotaxis pathway. *Sci. Signal.* **5**, ra2. (doi:10.1126/scisignal.2002413)
44. Weiner OD *et al*. 2006 Hem-1 complexes are essential for Rac activation, actin polymerization, and myosin regulation during neutrophil chemotaxis. *PLoS Biol.* **4**, e38. (doi:10.1371/journal.pbio.0040038)
45. Forsman H *et al*. 2013 Reactivation of desensitized formyl peptide receptors by platelet activating factor: a novel receptor cross talk mechanism regulating neutrophil superoxide anion production. *PLoS ONE* **8**, e60169. (doi:10.1371/journal.pone.0060169)
46. Omann GM, Sklar LA. 1988 Response of neutrophils to stimulus infusion: differential sensitivity of cytoskeletal activation and oxidant production. *J. Cell Biol.* **107**, 951–958. (doi:10.1083/jcb.107.3.951)
47. Sklar LA, Jesaitis AJ, Painter RG, Cochrane CG. 1982 Ligand/receptor internalization: a spectroscopic analysis and a comparison of ligand binding, cellular response, and internalization by human neutrophils. *J. Cell. Biochem.* **20**, 193–202. (doi:10.1002/jcb.240200210)
48. Inoue T, Meyer T. 2008 Synthetic activation of endogenous PI3K and Rac identifies an AND-gate switch for cell polarization and migration. *PLoS ONE* **3**, e3068. (doi:10.1371/journal.pone.0003068)
49. Zigmond SH, Levitsky HI, Kreel BJ. 1981 Cell polarity: an examination of its behavioral expression and its consequences for polymorphonuclear leukocyte chemotaxis. *J. Cell Biol.* **89**, 585–592. (doi:10.1083/jcb.89.3.585)
50. Ueda M, Sako Y, Tanaka T, Devreotes P, Yanagida T. 2001 Single-molecule analysis of chemotactic signaling in *Dictyostelium* cells. *Science* **294**, 864–867. (doi:10.1126/science.1063951)
51. Cassimeris L, McNeill H, Zigmond SH. 1990 Chemoattractant-stimulated polymorphonuclear leukocytes contain two populations of actin filaments that differ in their spatial distributions and relative stabilities. *J. Cell Biol.* **110**, 1067–1075. (doi:10.1083/jcb.110.4.1067)
52. Moores SL, Sabry JH, Spudich JA. 1996 Myosin dynamics in live *Dictyostelium* cells. *Proc. Natl Acad. Sci. USA* **93**, 443–446. (doi:10.1073/pnas.93.1.443)
53. Xu J *et al*. 2003 Divergent signals and cytoskeletal assemblies regulate self-organizing polarity in neutrophils. *Cell* **114**, 201–214. (doi:10.1016/S0092-8674(03)00555-5)
54. Fukui Y, Kitanishi-Yumura T, Yumura S. 1999 Myosin II-independent F-actin flow contributes to cell locomotion in dictyostelium. *J. Cell Sci.* **112**, 877–886.
55. Gerisch G, Albrecht R, Heizer C, Hodgkinson S, Maniak M. 1995 Chemoattractant-controlled accumulation of coronin at the leading edge of *Dictyostelium* cells monitored using a green fluorescent protein-coronin fusion protein. *Curr. Biol.* **5**, 1280–1285. (doi:10.1016/S0960-9822(95)00254-5)
56. Weiner OD, Servant G, Welch MD, Mitchison TJ, Sedat JW, Bourne HR. 1999 Spatial control of actin polymerization during neutrophil chemotaxis. *Nat. Cell Biol.* **1**, 75–81. (doi:10.1038/10042)